Original Article

The Role of Hypoxia on the Neuronal Differentiation of Gingival Mesenchymal Stem Cells: A Transcriptional Study

Cell Transplantation
2019, Vol. 28(5) 538–552

DOI: 10.1177/0963689718814470
journals.sagepub.com/home/cll
SAGE

Agnese Gugliandolo[1], Francesca Diomede[2], Domenico Scionti[1], Placido Bramanti[1], Oriana Trubiani[2], and Emanuela Mazzon[1]

Abstract

Mesenchymal stem cells (MSCs) are widely used in stem cell therapy for regenerative purposes. Oral-derived MSCs, such as gingival MSCs (GMSCs), deriving from the neural crest seem more suitable to differentiate toward the neuronal lineage. In addition, the preconditioning of MSCs may improve their beneficial effects. Since it is known that hypoxia may influence stem cell properties, we were interested in evaluating the effects of hypoxia preconditioning on the neuronal differentiation of GMSCs. With this aim, we evaluated the transcriptional profile of GMSCs exposed to basal and neuroinductive medium both in normoxia and in cells preconditioned for 48 h in hypoxia. We compared their transcriptional profile using Next Generation Sequencing. At first we observed that hypoxia did not alter cell morphology compared with the GMSCs cultured in a normoxic condition. In order to understand hypoxia preconditioning effects on neuronal differentiation, we screened genes with Log2 fold change $\geq$2 using the database Cortecon, that collects gene expression data set of in vitro corticogenesis. We observed that hypoxia preconditioning induced the expression of more genes associated with different stages of cortical development. The common genes, expressed both in normoxia and hypoxia preconditioning, were involved in developmental and neuronal processes. Interestingly, a larger number of genes associated with development biology and neuronal process was expressed in GMSCs differentiated after hypoxia preconditioning compared with those in normoxia. In addition, hypoxic-preconditioned differentiated GMSCs showed a higher expression of nestin, PAX6, and GAP43. Our data demonstrated that hypoxia preconditioning enhanced the differentiation potential of GMSCs and induced the activation of a higher number of genes associated with neuronal development. In conclusion, hypoxia may be used to improve MSCs' properties for stem cell therapy.

Keywords

mesenchymal stem cells, hypoxia, gingiva, neuronal differentiation, next generation sequencing

Introduction

Stem cell therapy appears to be a new good therapeutic strategy to treat different kinds of diseases[1,2]. In particular, mesenchymal stem cells (MSCs) are considered a promising approach to treat neurodegenerative disorders, in which progressive neuronal death is present and behavioral and cognitive functions decline as the disease progresses[2,3]. MSCs are known to differentiate toward mesodermal lineages, including bone[4], and also into endodermal and ectodermal tissues, such as neurons and glial cells[2]. Moreover, MSCs may exert beneficial actions through different mechanisms, such as neurogenesis and angiogenesis induction, inhibition of apoptosis, and immunomodulatory and anti-inflammatory effects[2,5]. Furthermore, most effects may be mediated in a paracrine manner, through the release of neurotrophic factors and cytokines. Beneficial actions have been reported in the treatment of different neurodegenerative diseases, both at molecular and behavioral levels, leading to an increase in the use of MSCs as therapeutic strategies in different aspects of human health[2].

Oral tissues, such as gingiva, represent a new abundant source of MSCs that permits a large amount of MSCs to be

[1] IRCCS Centro Neurolesi "Bonino-Pulejo", Messina, Italy
[2] Department of medical, oral and biotechnological sciences, University "G. d'Annunzio" Chieti-Pescara, Chieti, Italy

Submitted: August 10, 2018. Revised: October 30, 2018. Accepted: October 30, 2018.

Corresponding Author:
Emanuela Mazzon, IRCCS Centro Neurolesi "Bonino-Pulejo", Via Provinciale Palermo, Contrada Casazza, Messina 98124, Italy.
Email: emazzon.irccs@gmail.com

obtained with minimally invasive procedures and with no ethical issues[6,7]. Gingival MSCs (GMSCs), which show high regenerative potential and immunomodulatory properties, seem promising for the development of future therapeutic approaches, as already demonstrated in different therapeutic applications[7–10]. In addition, given their origin from the neural crest, they seem more useful for neuroregenerative purposes[7,11].

Different strategies are being researched in order to improve the efficiency of stem cell therapies. In particular, it is important to highlight that the oxygen (O_2) concentration used in in vitro culture is higher compared with the concentration to which tissues are exposed physiologically, even though this varies depending on the tissue type, varying from $\sim 1\%$ to $\sim 14\%$[12]. Indeed, when O_2 reaches the different tissues, its concentration drops to 2–9%, with a mean value of 3%[12,13]. For this reason different studies have investigated the effects of low O_2 concentrations (mainly in the range of 1–5%), showing that hypoxia influences MSC biology, including the growth, the differentiation potential, and the gene expression profile of MSCs[12,14]. For this reason, hypoxia preconditioning may influence and enhance the potential of MSCs for future cell-based therapy. It has already been shown that hypoxia may improve the immunomodulatory activity of GMSCs, increase skin wound repair in vivo, and promote the regenerative properties of GMSCs, suggesting that hypoxic preconditioning may be a good method to optimize the potential of GMSCs for tissue regeneration and stem cell therapies[15]. In addition, MSCs cultured under hypoxia (5% O_2 for 5 days) presented a higher proliferation rate, maintained higher levels of MSC surface markers, and expressed increased levels of Oct4, C-Myc, Nanog, nestin, and HIF-1α compared with cells under normoxic conditions[16]. However, whether hypoxia can ameliorate the differentiation potential of MSCs is still under debate, and contrasting results have been reported.

The aim of this study was to evaluate the influence of hypoxia preconditioning on neural differentiation of GMSCs. In particular, we performed Next Generation Sequencing analysis in order to assess the transcriptional changes induced by hypoxia preconditioning in cells induced to differentiate toward the neuronal lineage. For this purpose, we evaluated the transcriptional profile of GMSCs cultured in basal or neuroinductive medium in normoxia and after hypoxic preconditioning.

Materials and Methods

Isolation and culture of GMSCs

Written approval for gingival biopsy collection was obtained from the Medical Ethics Committee at the Medical School, "G. d'Annunzio" University, Italy, and each participant gave informed consent. Patients were free from from oral and systemic diseases. GMSCs were collected from healthy gingival tissue removed during surgical dentistry procedures. Gingival tissue was placed in MSCBM-CD (Lonza, Basel, Switzerland) and then incubated in a humidified atmosphere with 5% CO_2 at 37°C as previously described[17]. The medium was replaced every 3 days. After 2 weeks cells spontaneously migrated from the explants and the cells were maintained in MSCBM-CD (Lonza). Cells of passage 2 were used for all experiments.

Cytofluorimetric Evaluation

Antibodies . Fluorescein phycoerythrin-conjugated anti-CD29 (CD29 PE), and FITC-conjugated anti-CD44 (CD44 FITC), anti-CD45 (CD45 FITC), and anti-CD105 (CD105 FITC) were obtained from Ancell (Minnesota, USA); FITC-conjugated anti-CD14 (CD14 FITC) was purchased from Milteny Biotec (Bergisch Gladbach, Germany); PE-conjugated anti-CD73 (CD73 PE), FITC-conjugated anti-CD90 (CD90 FITC), PE-conjugated, Alexa488-conjugated anti-Sox2 (Sox2 Alexa488), FITC-conjugated anti-SSEA-4 (SSEA-4 FITC), and PE-conjugated anti-OCT3/4 (OCT3/4 PE) were obtained from Becton Dickinson (BD, Franklin Lakes, New Jersey, USA); PE-conjugated anti-CD31 (CD31-PE) and CD34 (CD34-PE) were purchased from Beckman Coulter (Brea, CA, USA); and an appropriate secondary FITC-conjugated antibody was obtained from Jackson Immunoresearch Laboratories (Cambridge House, Cambridgeshire, UK).

Washing buffer (phosphate-buffered saline, PBS, Sigma-Aldrich, Milan, Italy, 0.1% sodium azide, and 0.5% bovine serum albumin (BSA), VWR, Radnor, PA, USA) was used for all washing steps (3 ml of washing buffer and centrifugation, 400 *g* 8 min at 4°C). Briefly, 5×10^5 cells/sample were incubated with 100 ml of 20 mM ethylenediaminetetraacetic acid (EDTA, Sigma-Aldrich) at 37°C for 10 min and washed.

Staining of surface antigens and intracellular antigens was carried out according to Diomede et al[18]. 5×10^5 cells /sample were incubated with 100 ml of 20 mM EDTA at 37°C for 10 min. Cells were washed with 3 ml of washing buffer and centrifuged (4°C, 400× *g*, 8 min). For surface antigens, samples were resuspended in 100 ml washing buffer containing the appropriate amount of surface antibodies, incubated for 30 min at 4°C in the dark, washed (3 ml of washing buffer), centrifuged (4°C, 400× *g*, 8 min), resuspended with 1 ml 0.5% paraformaldehyde, incubated for 5 min at room temperature (RT), washed, centrifuged (4°C, 400× *g*, 8 min), and stored at 4°C in the dark until acquisition. For intracellular antigens, samples were resuspended in 1 ml of FACS lysing solution (BD), vortexed, and incubated at RT in the dark for 10 min. Samples were centrifuged (4°C, 400× *g*, 8 min); 1 ml of Perm 2 (BD) was added to each tube and cells were incubated at RT in the dark for 10 min. Samples were washed and centrifuged (4°C, 400× *g*, 8 min). Cells were resuspended in 100 ml of washing buffer containing the appropriate amount of intracellular antibodies and incubated for 30 min at 4°C in the dark. Cells were centrifuged (4°C, 400× *g*, 8 min), resuspended with 1 ml 0.5%

paraformaldehyde, incubated for 5 min at RT, washed, centrifuged (4°C, 400× *g*, 8 min) and stored at 4°C in the dark until the acquisition. Cells were analyzed on a FACSCalibur flow cytometer (BD), using CellQuestTM software (BD). Quality control included regular check-ups with Rainbow Calibration Particles (BD). Debris was excluded from the analysis by gating on morphological parameters; 20,000 non-debris events in the morphological gate were recorded for each sample. To assess non-specific fluorescence we used isotype controls. All antibodies were titrated under assay conditions and optimal photomultiplier voltages were established for each channel[19]. Data were analyzed using FlowJoTM software (TreeStar, Ashland, OR, USA).

Cell Treatment and Neuronal Differentiation

GMSCs were cultured in normoxic (N) (21% O_2) or under hypoxic (H) conditions (3% O_2). After 48 h of culture, GMSCs under hypoxic conditions were induced to neurogenic differentiation; GMSCs maintained in normoxic conditions were also induced to the same differentiation.

Neuronal induction was performed by the method described elsewhere[20,21]. Briefly, an appropriate amount of passage 2 cells was plated at 2×10^3 cells/cm^2 in an 8-well chamber-slide culture dish. Then neuronal induction medium, consisting of Neurobasal-A Medium (Gibco, Waltham, MA, USA) containing B27 (2%), L-glutamine (2 mM), penicillin (100 U/ml), streptomycin (100 mg/ml) and amphotericin B (5 mg/ml) (neuroinductive medium) and supplemented with basic fibroblast growth factor (bFGF, 20 ng/ml) (TemaRicerca, Milan, Italy), was added. The induction was maintained for 10 days, after which cells were processed for further evaluations.

Immunofluorescence

All samples were treated to highlight neurogenic-specific markers for subsequent observation with confocal laser scanning microscopy. The primary antibodies were mouse anti-GAP43 (1:100; Sigma Aldrich, Milan, Italy) and rabbit anti-Nestin (1:200; Santa Cruz Biotechnology, Dallas, TX, USA). Samples were incubated with secondary antibodies Alexa Fluor 488 (Molecular Probes, Life Technologies, Monza, MI, Italy) at RT for 1 h[22]. All samples were incubated with Alexa Fluor 568 phalloidin red fluorescence conjugate (1:400) to stain the cytoskeleton actin and with TOPRO to stain nuclei[23]. Samples were observed by means confocal laser scanning microscopy (Zeiss LSM800 META, Zeiss, Jena, Germany).

Western Blot Analysis

Undifferentiated and differentiated GMSCs in normoxic and hypoxic conditions were seeded on 6-well plates. At the end of the treatment cells were collected and centrifuged for 8 min at 980 rpm and the pellet was lyzed in RIPA buffer (Thermo Fisher Scientific, Waltham, MA, USA) plus 10% of protease inhibitor cocktail (Roche Molecular Diagnostics, Pleasanton, CA, USA).

40 micrograms of total proteins were diluted in Bolt® LDS Sample Buffer (Life Technologies), added with Bolt® Sample Reducing Agent (Life Technologies) and heated at 95°C for 5 min. Samples and molecular weight markers were separated on Bolt™ 4–12% Bis-Tris Plus Gels and transferred to PVDF membrane using the iBlot® 2 Gel Transfer Device (Life Technologies). After a blocking step using NFDM 5% in PBS 1× plus Tween-20 0.1% for 2 h at RT, blots were washed three times in PBS and the membranes were incubated overnight at 4°C with mouse anti-PAX6 antibody (Merck-Serono, Milan, Italy) at the appropriate dilution (1:500). The next day blots were washed with PBS 1× plus Tween-20 0.1% and reacted with the secondary antibody goat anti-mouse (Bethyl Laboratories, Montgomery, AL, USA) for 1 h. Membranes were washed again three times with PBS 1× plus Tween-20 0.1% and immunocomplexes were visualized using the enhancing chemiluminescence detection reagent Luminata Crescendo (Millipore, Merck Group, Milan, Italy), and digital scans were obtained with the Alliance 9.7 system (UVItec Limited, Cambridge, UK)[24]. To determine the equal loading of samples per lane, at the end of each experiment the blots were stripped with ReBlot Plus Strong Antibody Stripping Solution (Merck, Vimodrone, MI, Italy) and reprobed with rabbit anti β-actin polyclonal antibody (Santa Cruz Biotechnology, Santa Cruz, CA, USA), according to the manufacturer's instructions. Protein bands were quantified through the computer program ImageJ software. Statistical analysis was performed with GraphPad Prism version 7.0 software (GraphPad Software, La Jolla, CA, USA), using one-way ANOVA test and Bonferroni post-hoc test for multiple comparisons. A P value less than or equal to 0.05 was considered statistically significant. Results are reported as mean ± SEM.

RNA Extraction

Total RNA was extracted from all samples using the RNeasy Mini Kit (Qiagen, Hilden, Germany) and quantified by means of a BioSpectometer (Eppendorf, Milan, Italy)[25].

Illumina cDNA Library Construction

Library construction was performed according to the TruSeq RNA Access library Prep kit protocol (Illumina, San Diego, CA, USA). Following the protocol, 40 ng of total RNA was fragmented in a thermal cycler at 94°C for 8 minutes, and used for first strand cDNA synthesis by SuperScript II reverse transcriptase activity (Invitrogen, Carlsbad, CA, USA). The double-strand cDNA was synthesized through incubation at 16°C for 1 h with Second Strand Marking Master Mix (Illumina). Subsequently a purification step was carried out using AMPure XP beads with the aim to

eliminate the reaction mix components. By fragment adenylation at the 3' ends, the ligation of complementary adapters (showing a "T" nucleotide to the 3' ends) is possible, together with a reduced rate of chimera (concatenated template) formation. After this, Adapter-Indexes ligation to the double-strand cDNA fragment allows the identification of each sample, and it is necessary to prepare them for hybridization on the flow cell. After a clean-up step, a first PCR amplification was carried out as stated: initial denaturation at 98°C for 30 s, 15 cycles consisting of 98°C for 10 s, 60°C for 30 s, 72°C for 30 s, and final extension at 72°C for 5 min. A first hybridization reaction allows mixing of the cDNA library with exome capture probes with the aim of selecting and enriching specific regions of interest. The hybridization reaction (95°C for 10 min, 18 cycles of 1 min incubation, starting at 94°C, decreasing 2°C per cycle and 58°C for 90 min) allows us to obtain a pool of different indexing libraries, by using 200 ng of each one. Streptavidin-conjugated magnetic beads were used in order to purify sample pool. A second hybridization step and another streptavidin purification step were carried out. A final PCR amplification (98°C for 30 s, 10 cycles: 98°C for 10 s, 60°C for 30 s, and 72°C for 30 s, and 72°C for 5 min) was then performed and followed by a clean-up. The library was qualitatively and quantitatively validated by Bioanalyzer instrument (Agilent High Sensitivity DNA Kit, Richardson, TX, USA) and Real-Time PCR (KAPA Library Quantification Kit-Illumina/ABI Prism®, Kapa Biosystems, Wilmington, MA, USA), respectively. The library was denatured by 2 N NaOH and diluted until 12 pM concentration. MiSeq Reagent Kit v3 (600 cycles) was used for sequencing on the MiSeq Instrument (Illumina), by setting a single read. Experiments were carried out in triplicate.

MiSeq-Generated Data Processing and Statistical Analysis

The CASAVA software version 1.8 (Illumina) was used for generating the "Fastaq.File". The file.fastaq were aligned using the tool STAR version, and the "homo sapiens UCSC hg19" reference sequence was used for mapping. In order to evaluate the rate of differentially expressed genes between the different experimental groups that were statistically significant, a statistical analysis was performed with the Cufflinks Assembly & DE package version 2.0.0. q value ≤ 0.05 was considered statistically significant.

In order to normalize and compare the samples, the FPKM value (fragments per kilobase of exon per million fragments mapped) was calculated by applying the mathematical formula: (1000 $\times$ read count) / (number of gene covered bases $\times$ number of mapped fragments in million). A scatter plot of the Log2 of the FPKM was used in order to compare the two experimental groups. Gene Ontology (GO) (http://www.geneontology.org/), Cortecon (http://cortecon.neuralsci.org/), and REACTOME (https://reactome.org/) were used to investigate and screen the differentially expressed genes between the experimental groups. Only significant GO were considered in this work (FDR $P < 0.05$).

Results

Cytofluorimetric and Morphological Analysis of GMSCs

The cell phenotypic characteristics were detected by flow cytometry analysis through the testing of negativity for CD14, CD31, CD34, and CD45, and positivity for CD29, CD44, CD73, CD90, and CD105, and for mesenchymal markers Oct3/4, Sox-2, and SSEA4 (Fig. 1B).

Morphological evaluation of GMSCs cultured in normoxic and hypoxic conditions was carried out by means confocal laser scanning microscopy observations. Cells cultured with basal medium in normoxic (CTR-N) and hypoxic (CTR-H) conditions showed a fibroblast-like morphology, with long cytoplasmic processes (Fig. 1 A1, A3). Meanwhile, cells induced to neurogenic differentiation changed their typical morphological aspect, showing an actin rearrangement both for GMSC growth under normoxic (DIFF-N) or hypoxic preconditioning (DIFF-H) (Fig. 1 A2, A4).

Global Transcriptome Analysis

We first compared CTR-N and DIFF-N. We observed that 4392 genes were differentially expressed, of which 2318 were up-regulated in DIFF-N, while 2074 were down-regulated (Fig. 2A).

Comparing the transcriptional profile of CTR-H and DIFF-H we found that 4562 genes were differentially expressed. Among these genes, 2372 genes were up-regulated in DIFF-H, while 2190 genes showed a down-regulation of their expression (Fig. 2B).

GO analysis revealed the significant involvement of the biological processes "Cellular process," "Biological regulation," and "Metabolic process," but also processes linked to development, such as "Developmental process," "System development," and "Nervous system development" (Fig. 3). Furthermore, the processes "Cell differentiation," "Neurogenesis," and "Neuron differentiation" were also significantly represented (Fig. 3).

Analysis of Differentially Expressed Genes using Cortecon

In order to evaluate the involvement of differentially expressed genes in nervous system development, we screened the genes with Log2 fold change ≥ 2 using the online database Cortecon. This database collects the temporal gene expression dataset of in vitro corticogenesis from human embryonic stem cells, identifying genes and long noncoding RNAs that significantly change during cortical development. Genes are associated in clusters, and each cluster is associated with one or more stages of cortical development[26].

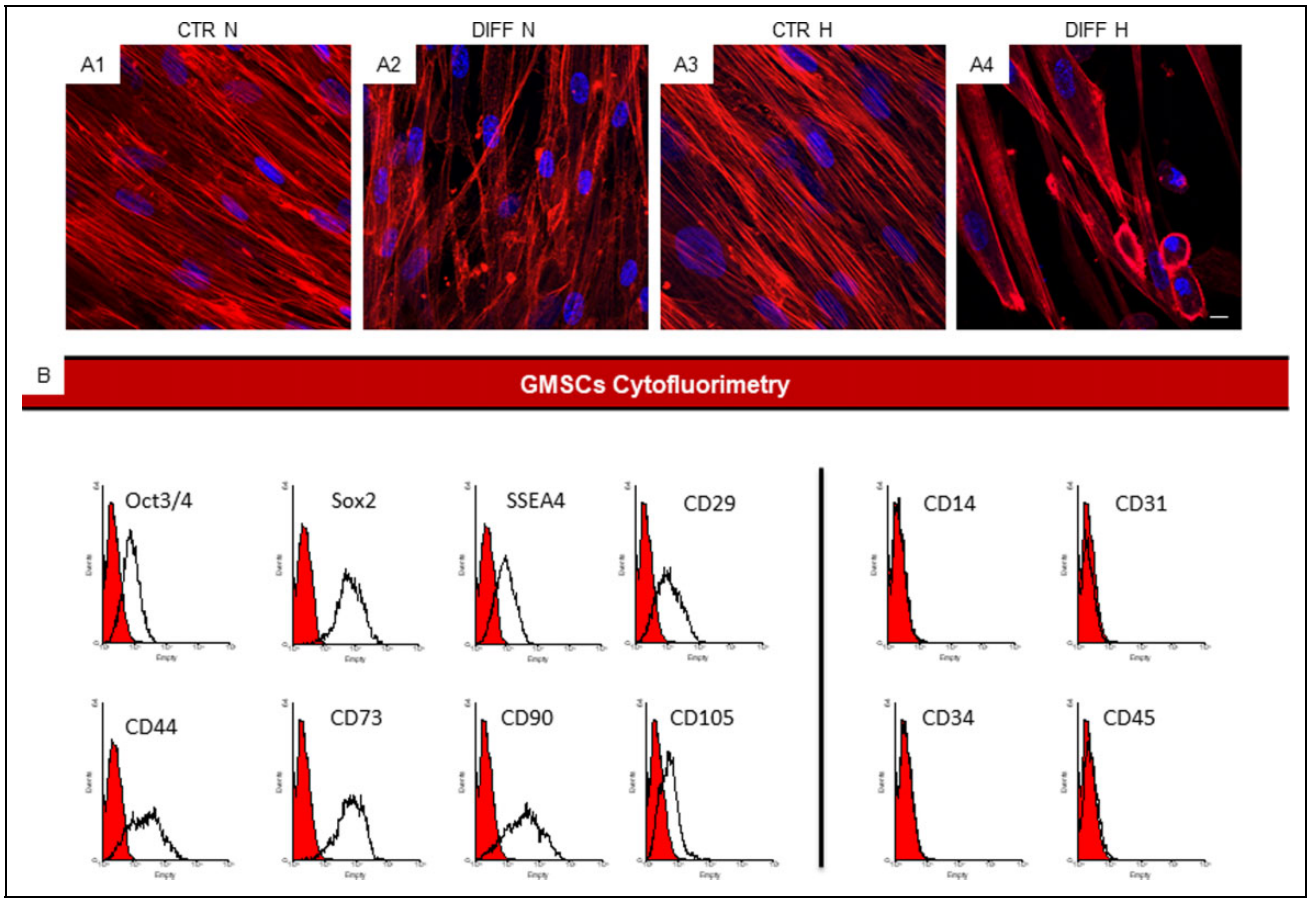

Fig. 1. Morphological and immunophenotyping of GMSCs. Immunofluorescence staining of GMSCs cultured under normoxic conditions in (A1) basal medium and in (A2) neurogenic differentiated medium. Immunofluorescence staining of GMSCs cultured under hypoxic conditions in (A3) basal medium and in (A4) neurogenic differentiated medium. Red fluorescence: cytoskeleton actin. Blue: nuclei. Scale bar: 5 μm. (B) Immunophenotypic analysis of GMSCs. GMSCs expressed Oct ¾, Sox-2, SSEA-4, CD29, CD44, CD73, CD90, and CD105 but not CD14, CD31, CD34, or CD45.

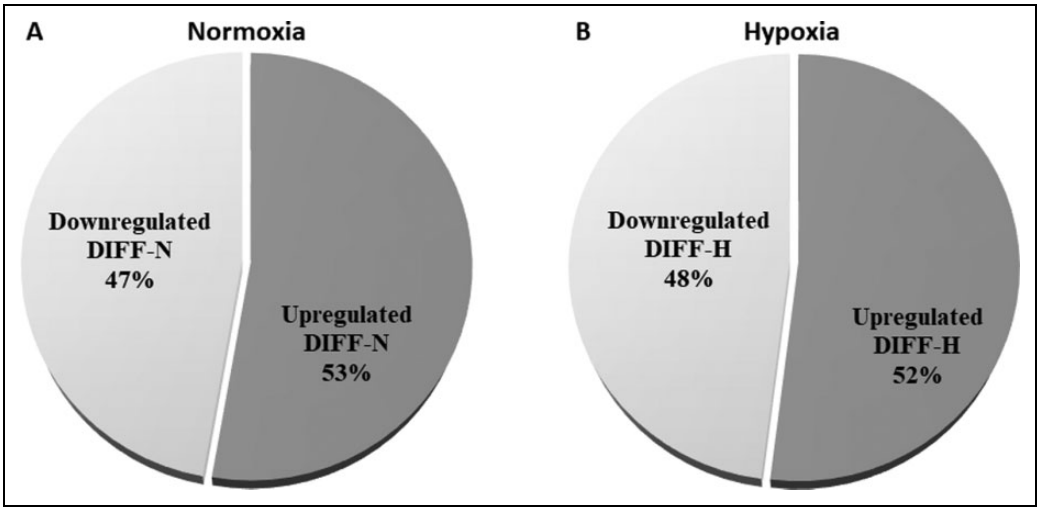

Fig. 2. Global transcriptomic analysis. (A) Genes up-regulated and down-regulated in GMSCs differentiated under normoxia. (B) Genes up-regulated and down-regulated in GMSCs differentiated after hypoxia preconditioning. Transcriptomic analysis revealed that both in normoxic and hypoxic conditions, differentiated GMSCs showed a higher number of up-regulated genes.

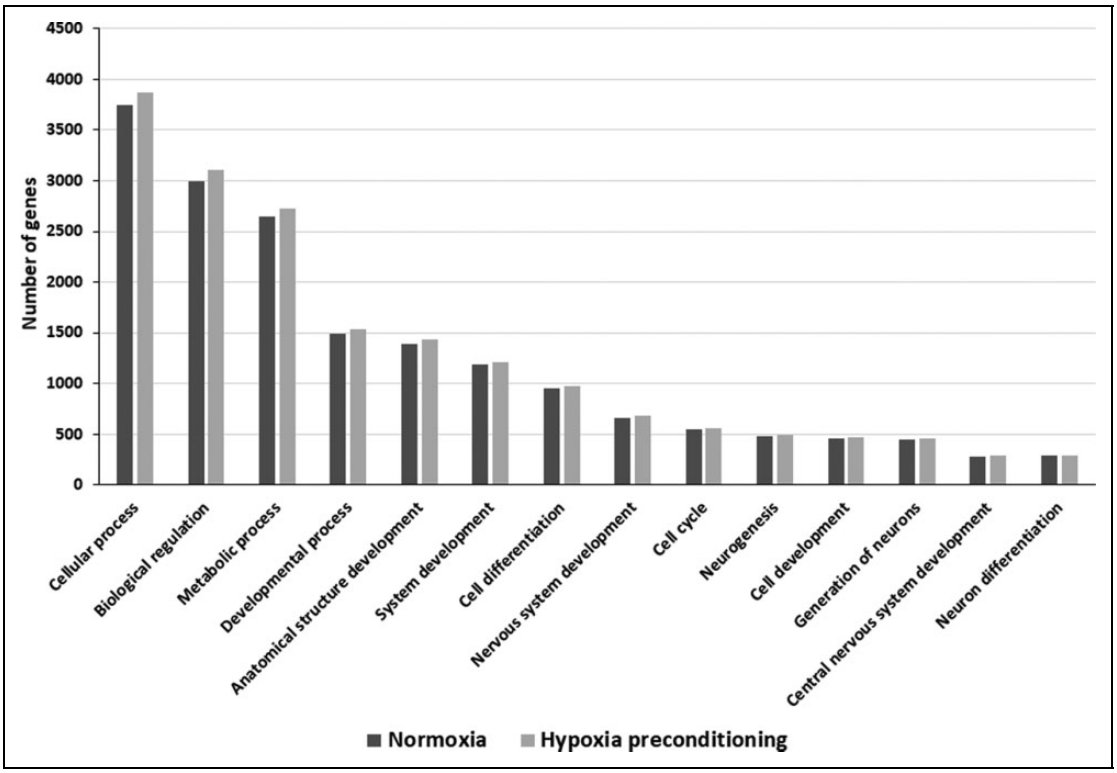

Fig. 3. Gene ontology analysis. The analysis evidenced that among the significant biological processes were those involved in development and differentiation.

At first we noticed that the GMSCs preconditioned with hypoxia showed a higher number of genes with Log2 fold change $\geq$2. In particular, comparing CTR-N and DIFF-N, we found 591 genes with Log2 fold change $\geq$2, and screening them with Cortecon we found that 420 were associated with the different stages of cortical development. Regarding CTR-H and DIFF-H, 729 genes presented Log2 fold change $\geq$2, and of these 503 were involved in at least one stage of corticogenesis. We then evaluated the genes selected with Cortecon, dividing them into common genes, which were expressed both in cells cultured in normoxia and in hypoxia-preconditioned GMSCs, and those expressed in cells preconditioned with hypoxia or in the normoxic condition. We found that 254 genes were commonly expressed (Table 1), and 249 were expressed in GMSCs preconditioned with hypoxia with Log2 fold change $\geq$2 (Table 2 and Table S1), while 166 genes were expressed in GMSCs cultured in normoxia with Log2 fold change $\geq$2 (Table 3 and Table S2).

We evaluated which stage of differentiation was the most represented first for the common genes. We observed that the highest number of genes was included in clusters associated with the "cortical development" stage, followed by the "pluripotency" stage. Indeed, the most represented clusters were the numbers 14, associated with the "cortical specification" stage, and 31 that included genes involved in "pluripotency." Among the 166 genes expressed in GMSCs in normoxia, the majority belonged to clusters associated with pluripotency and cortical specification. The most represented clusters were 42, associated with "pluripotency" and "cortical specification", and 14 and 15, associated with "pluripotency."

Considering the genes expressed in GMSCs preconditioned in hypoxia the most represented stages were "cortical specification" and "pluripotency," with almost an equal number of genes. The clusters with the biggest number of genes were 14 and 15. It is interesting to note that the common genes showed a similar fold change for both GMSCs differentiated with/without hypoxia preconditioning.

In order to better understand the role of these genes, we characterized them through GO analysis (Fig. 4).

Considering the common genes expressed during differentiation in both GMSCs cultured in normoxic and after hypoxic preconditioning, GO analysis revealed the association with the biological process categories "Cellular process," "Metabolic process," and "Developmental process," including "Nervous system development" (Fig. 4). Looking at the genes expressed during differentiation in normoxia or in hypoxia-preconditioned GMSCs, the most represented GO process was "Cellular process" in each condition, followed by categories linked to metabolic processes (Fig. 4). Interestingly, in GMSCs differentiated after hypoxic preconditioning, among the significant GO processes we observed "regulation of dendrite development" (Fig. 4).

Table 1. Common Genes Expressed in Control and Differentiated GMSCs Cultured in Normoxia and After Hypoxia Preconditioning Screened Through the Database Cortecon, and the Associated Stages of Development.

DATA Cortecon	Genes
Pluripotency	HIST1H3 J, ZNF431, HIST1H2BE, NUP205, ADM, TXNL4A, FAM104A, PCK2, MCM7, FARSB, KPNA2, RECQL, KLF5, FOXRED1, GRPEL1, TUBB2A, NDUFAF2, PLP2, SMS, TAGLN, TPM3, NME1, CBS, IMPDH2, HSPD1, CDC37, FKBP1A, HNRNPF, ACLY, ARPC5 L, LRRC59, PSMC3, ATL3, TAF15, NDUFV2, NT5DC2, TMBIM1, PRELID1, SRPX, SYNJ2, XBP1, KIF1C, PSMD2, CCM2, RPS5, EMP3, APRT, FADS2, PTGES3, PYCR1, IARS, YBX1, ZWILCH, TXNDC17, GLRX3, KPNB1, FLNA, G3BP1, PDIA4, SDHB, THY1, SNRPG, ACSL3, ARPC1A, PGK1, ATP5B, RPS16, CD248, INTS7, MYL6, TALDO1, RBPMS, ECHDC1, ADI1, BAG5, HIATL1, SMARCAL1, RRAS2, MIS18BP1, TNFAIP6, SUPT16 H, GFM1, POLG, FAM49B, PSMD11, ETV1, PRPF4, PLS3, PHLDA1, ATAD3A, YES1, CYCS, TM7SF3, ACO1, PFAS, GPR176, RFC2, MT1 L, SLC38A1, NCAPH, HIST1H3G, TOP2A, FOXC2, CCNB1, WEE1, ZIK1, NCAPH2, COQ2, CCNA2, TIMP4, WDR75, TTLL5, NCAPG2, HSPA2, EZH2, SLC29A1, MAD2L1, TACC3, AURKA, LRR1, TRIP13, RFC3, GPR89A, TUBA1C, ESPL1, TK1, FKBP5
Neural Differentiation	NUSAP1, HIST1H3B, HIST1H2BJ, TSC22D3, HIST1H2BG, H1FX, GLUL, ITGA5, ZFHX3, COL11A1, EMP1, HIPK1, NR1D1, SMOC1, HNRNPA0, SULF1, FOS, BACH1, NID2, NOTCH2, LZTR1, ZNF441, SPOCK1, PTMS, AKR1C2, ODF2, SNAI2, ARNT, ZEB1, RRAS, VPS28, ARID5B, PLEKHA4, CCDC80, GSN, ATP6AP2, TMEM98, GLI3, MAGED2, MAP3K12, LTBP4, ROBO1, DNM1, DNASE2, DMPK, DDHD2, PTPRU, SCD5, KLHL5, HMGB2, HIST1H2AE, RNASEL, MAMLD1, CDAN1, HIST1H2 AD, HIST1H3D, PER2, HIST3H2A, KLF4, HSD17B14
Cortical Specification	HIST1H3 J, HIST1H3B, NUP205, RACGAP1, HIST1H2BJ, TSC22D3, HIST1H2BG, HIST1H2BN, H1FX, MCM7, PTTG1, KPNA2, RECQL, KLF5, FBXW5, ZFHX3, COL11A1, KIF11, PLP2, EMP1, HIPK1, H2AFJ, NR1D1, PCYOX1, NME1, SAMHD1, FBN2, LRRC59, SULF1, FOS, KDELR2, PTGES3, PYCR1, YBX1, NID2, NOTCH2, SPON2, PDIA4, COPZ2, SNRPG, LZTR1, CENPE, PGK1, ZNF441, HM13, RBM43, CD248, MYOF, SPOCK1, PTMS, MYL6, ECHDC1, LAMA3, PPIG, BAG5, CERCAM, ODF2, SNAI2, ARNT, ZEB1, RRAS, VPS28, ARID5B, SLIT3, PLEKHA4, CCDC80, GSN, ATP6AP2, DDX24, NPC2, AES, HEXB, SUPT16 H, GFM1, GLI3, MAN1A1, MAGED2, ETV1, SMARCA2, CCDC69, MMP14, IGFBP6, BTN3A3, SERPINF1, PLS3, LTBP4, ITM2B, LGALS3BP, TANC1, DNASE2, DMPK, DDHD2, PTPRU, SCD5, RFC2, KLHL5, ACSL4, MKI67, NDC80, RNASEH2A, FANCI, KIF4A, TOP2A, CCNB1, HIST1H3 H, CKS1B, PORCN, NUBP1, CADM1, HIST1H2AE, WEE1, RNASEL, MAMLD1, DNAJC9, CCNA2, HIST1H2 AD, TTLL5, HIST1H3D, NCAPG2, KIF14, KIF2C, PER2, MAD2L1, ARHGAP11B, TACC3, AURKA, ELN, HIST3H2A, CENPF, SPC24, TUBA1C, UBE2C, H2AFX, KLF4, HSD17B14, RNASE4, ESPL1
Upper Layers	HIST1H2BJ, TXNL4A, TSC22D3, HIST1H2BG, KLF5, GLUL, FBXW5, COL11A1, PLP2, EMP1, HIPK1, H2AFJ, NR1D1, PCYOX1, SAMHD1, HNRNPF, SULF1, ATL3, FOS, SRPX, PENK, EMP3, PYCR1, NID2, SPON2, PDIA4, COPZ2, LZTR1, ZNF441, RBM43, CD248, MYOF, AKR1C2, KCNMA1, LAMA3, ADI1, CERCAM, HIATL1, ODF2, VPS28, ARID5B, SLIT3, PLEKHA4, CCDC80, GSN, ATP6AP2, TMEM98, DDX24, AES, HEXB, IFITM3, MAN1A1, MAGED2, MAP3K12, SMARCA2, CCDC69, MMP14, IGFBP6, BTN3A3, KCNK2, SERPINF1, PLS3, PHLDA1, ITM2B, LGALS3BP, SCN9A, DNM1, TANC1, DNASE2, PTPRU, SCD5, HIST1H3 H, PORCN, CADM1, HIST1H2AE, RNASEL, MAMLD1, CDAN1, HIST1H2 AD, TTLL5, HIST1H3D, PER2, ELN, HIST3H2A, KLF4, RNASE4
Deep Layers	HIST1H2BE, HIST1H2BB, HIST1H2BJ, HIST1H2BF, TSC22D3, HIST1H2BN, KLF5, GLUL, FBXW5, NDUFAF2, ZFHX3, COL11A1, PLP2, EMP1, SMS, HIPK1, H2AFJ, NR1D1, PCYOX1, FBN2, IMPDH2, CDC37, EIF4G3, LRRC59, SULF1, IER5, XBP1, KDELR2, RPS5, FADS2, PYCR1, NID2, NOTCH2, PDIA4, COPZ2, ACSL3, LZTR1, PGK1, ZNF441, HM13, ATP5B, RPS16, CD248, MYOF, SPOCK1, AKR1C2, BAG5, CERCAM, ODF2, LAMB2, ARNT, ZEB1, SBF2, RRAS, VPS28, ARID5B, CCDC80, GSN, ATP6AP2, TMEM98, DDX24, NPC2, AES, GFM1, POLG, WNT5A, MAN1A1, MAGED2, MAP3K12, PRPF4, SMARCA2, CCDC69, MMP14, BTN3A3, SERPINF1, PLS3, LTBP4, ITM2B, LGALS3BP, YES1, TM7SF3, TANC1, DNASE2, DMPK, PTPRU, SCD5, KLHL5, HIST1H3G, FOXC2, PORCN, CADM1, RNASEL, HIST1H2 AD, TTLL5, PER2, ELN, HIST3H2A, KLF4, RNASE4

We also performed REACTOME screening to evaluate the genes belonging to processes related to developmental biology and the neuronal system. Some common genes were involved in developmental biology, and in particular in the sub-processes "Activation of HOX genes during differentiation," "Activation of anterior HOX genes in hindbrain development during early embryogenesis," and "axon guidance" (Table 4). In addition, five genes belonged to neuronal system processes (Table 4) and to the pathways "Transmission across chemical synapses" and its subpathways, and to "Potassium channel."

Analyzing the genes expressed after hypoxic preconditioning, we observed that three genes belonged to neuronal system pathways (Table 5). On the contrary, in cells cultured in normoxia, only two genes were present in neuronal system pathways (Table 6). Furthermore, we observed more genes belonging to developmental biology in GMSCs after hypoxic preconditioning compared with those in normoxic conditions. In particular, after hypoxic preconditioning, eight genes belonging to axon guidance were up-regulated; on the contrary, only one was up-regulated in GMSCs in the normoxic condition (Table 5 and 6).

Immunofluorescence Analysis

In order to investigate how hypoxic preconditioning influenced the expression of specific neurogenic markers, immunofluorescence staining was performed. The

Table 2. Genes Expressed in GMSCs Preconditioned in Hypoxia with Log2 Fold Change ≥5 Screened Through the Database Cortecon, Their Expression Values, the Associated Clusters and Stages of Development.

Gene	CTR-H	DIFF-H	LFC	q value	DATA Cortecon	Cluster
GINS2	0,0001	6,56029	16,00147197	0.00021023	P	27
OAS1	0,0284	11,76957	8,694954968	0.0113107	UL	58
LRRC37B	0,03849	7,82168	7,666851032	0.00040247	ND, CS, DL	21
HIGD1A	0,13244	23,6862	7,482564038	0.00021023	CS, DL	46
ILKAP	0,06475	11,32078	7,449877455	0.0204032	P	22
HECTD3	0,09363	12,98171	7,11529386	0.0381442	P, DL	47
MPHOSPH9	0,09211	7,40113	6,328243955	0.0157178	P	27
MCM3	0,12624	8,5516	6,081953357	0.00021023	P	15
B3GAT3	0,25377	15,48362	5,931077468	0.0317858	ND, DL, UL	23
MAEA	0,38011	23,0657	5,923188286	0.00927348	P, UL	35
NOP16	0,07177	4,33224	5,915588438	0.021626	P	22
MCMBP	0,29276	16,88121	5,849556055	0.00021023	P	15
MPV17L2	0,1721	9,76548	5,826371956	0.0015914	P, DL	47
RIPK1	0,28543	15,95988	5,805169017	0.023779	P, CS, DL, UL	57
SYNE2	0,061558	3,4088	5,791173787	0.00021023	UL	39
USP15	0,23634	12,28666	5,700085154	0.0179783	P	22
CEP78	0,19785	8,49749	5,424557789	0.0023455	ND	41
GALE	0,37511	15,88979	5,404642524	0.00817159	P, DL	60
RNF34	0,38539	15,6352	5,342334726	0.00605902	P	50
DAGLA	0,22385	8,74409	5,287704027	0.0232816	P, UL	35
KCTD1	0,23984	9,32374	5,280764581	0.000764474	DL	11
ANKLE2	0,29992	11,0417	5,202240768	0.00021023	P	5
NOL12	0,21472	7,46545	5,119700744	0.00655879	P	15
SAMD10	0,264493	9	5,088623555	0.0232816	CS, UL, DL	45
KPNA3	0,12263	4,11237	5,067586207	0.00605902	P	22
PCMTD1	0,45468	15,0682	5,050511731	0.00127075	ND, CS, DL, UL	4
TIMELESS	0,43063	14,07079	5,030110691	0.00021023	ND, DL	25
PLEKHO2	0,41945	13,66731	5,026086663	0.0448148	P	5
TEAD3	0,46532	15,03217	5,01368628	0.000936756	CS	14
ENDOV	0,2385	7,69273	5,011434502	0.00021023	ND, CS, UL	40
CNTN3	0,220481	7,0948628	5,008048544	0.0179783	CS, UL, DL	17

P: Pluripotency; CS: Cortical Specification; ND: Neural Diff; DL: Deep Layers; UL: Upper Layers; LFC: Log2 Fold change.

immunofluorescence results demonstrated the expression of GAP43 and nestin in DIFF-N and DIFF-H (Fig. 5). Compared with the undifferentiated GMSCs, the expression of GAP43 and nestin was significantly increased in the differentiated GMSCs, especially in DIFF-H.

Western Blot Analysis

Western blotting showed that neurogenic differentiation increased PAX6 protein levels both in GMSCs in normoxia and in hypoxia-preconditioned cells compared with the respective controls. Moreover, the stimulation in hypoxic conditions enhanced the expression of PAX6 in GMSCs induced to neurogenic differentiation when compared with GMSCs cultured in normoxia conditions with neuronal medium (Fig. 6).

Discussion

Different strategies have been developed in order to promote neurogenesis and regeneration[27,28]. Moreover, in the field of stem cell therapy, the preconditioning of MSCs, culturing them in specific conditions or through the addition of different compounds, may improve their efficacy. In particular, hypoxia influenced MSCs' properties, and preconditioning cells with low O_2 concentrations seems to enhance the biological actions of MSCs. Indeed, physiologically, tissues are exposed to O_2 concentrations (about 2–9%[12,13]) lower than those used in vitro.

A type of dental MSC, dental pulp stem cells (DPSCs), grown in a hypoxic condition were found to be smaller and have bigger nuclei. DPSCs cultured with 5% O_2 showed a significant enhancement of proliferation and migration, and an increased expression of the stem cell markers and of the genes SOX2, VEGF, NGF, and BDNF, indicating an improvement of MSC properties[29].

Our results provide evidence that hypoxia did not induce changes in morphology in CTR-H; GMSCs showed the classical fibroblast-like morphology. Both differentiated GMSCs, either DIFF-N and DIFF-H, showed actin rearrangements with morphological changes. It is known that changes in actin cytoskeleton happen during neurogenesis,

Table 3. Genes Expressed in GMSCs Cultured in Normoxic Condition with Log2 Fold Change ≥5 Screened Through the Database Cortecon, their Expression Values, the Associated Clusters and Stages of Development.

Gene	CTR-N	DIFF-N	LFC	q_value	DATA Cortecon	Cluster
DLGAP5	0,03	22,21	9,46	0.00021023	CS	14
HIST1H3E	0,03	16,89	9,27	0.0412378	ND, CS, UL	40
NPAS2	0,01	3,75	8,60	0.00021023	CS, DL, UL	30
EBF3	0,04	6,18	7,12	0.000586124	CS, UL	28
SRGAP3	0,05	5,34	6,89	0.00021023	ND, CS, DL, UL	2
MRPL44	0,06	7,54	6,88	0.0266573	P, DL	47
POC1A	0,08	7,56	6,54	0.00021023	P	50
ADRA2A	0,06	5,29	6,42	0.00021023	CS, DL, UL	30
CENPI	0,11	8,38	6,27	0.00021023	P, CS	42
DHX35	0,05	3,20	6,04	0.0288066	P	27
GALNT6	0,21	12,23	5,87	0.00021023	P	31
NR2C1	0,14	7,97	5,86	0.0295505	ND	41
MXI1	0,13	7,03	5,80	0.000586124	ND, CS, DL	33
WISP1	0,15	7,61	5,63	0.00021023	CS, DL, UL	24
CMKLR1	0,20	9,17	5,54	0.00021023	P	5
TMEM237	0,15	6,61	5,43	0.00348728	ND	37
FZD1	0,29	10,49	5,19	0.00021023	ND, CS, DL, UL	4
TDP1	0,33	11,79	5,15	0.00021023	P	50
CDKN3	0,66	22,79	5,10	0.00021023	CS	14

P: Pluripotency; CS: Cortical Specification; ND: Neural Diff;DL: Deep Layers; UL: Upper Layers; LFC: Log2 Fold change.

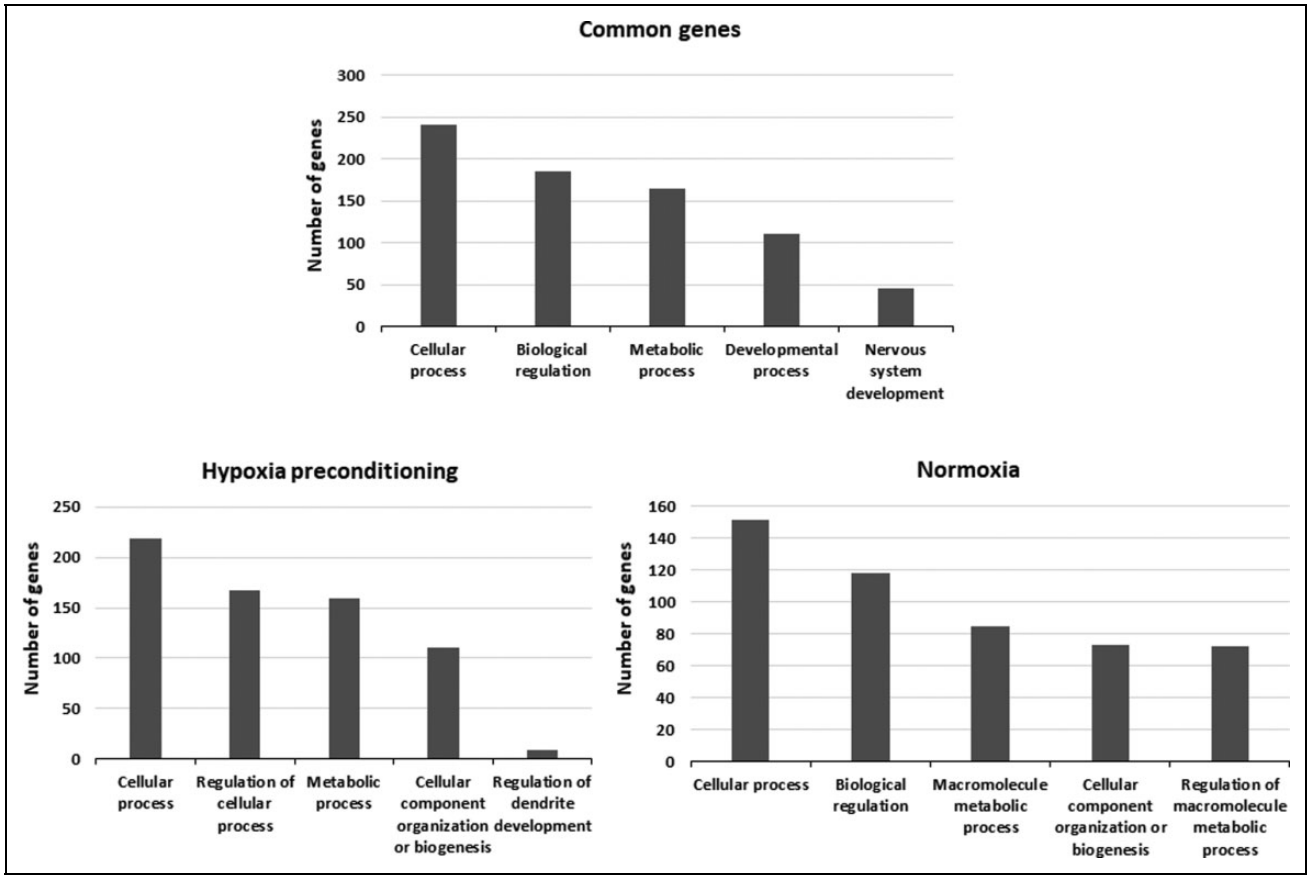

Fig. 4. Gene ontology analysis of genes screened by Cortecon.

Table 4. Common Differentially Expressed Genes Belonging to REACTOME Pathway Related to Developmental Biology and Nervous System.

Pathways	Genes
Developmental biology, Activation of HOX genes during differentiation, Activation of anterior HOX genes in hindbrain development during early embryogenesis	HIST1H2BN, HIST1H3D, HIST1H2BB, EZH2, HIST1H3B, HIST1H3 J, HIST1H3 H, HIST1H2BE, HIST1H3G, HIST1H2BG, H2AFJ, H2AFX, HIST1H2AE, HIST1H2 AD, HIST1H2BJ, HIST1H2BF
Developmental biology	MAMLD1, KLF5, KLF4
Developmental biology, Axon guidance	DNM1, YES1, PSMD11, ARPC1A, TUBA1C, PSMD2, RRAS, PSMC3, TUBB2A, ITGA5, MYL6, RPS16, SCN9A, RPS5, ROBO1, SLIT3, KIF4A
Neuronal system, Transmission across chemical synapses, Neurotransmitter uptake and metabolism in glial cells	GLUL, SLC38A1
Neuronal system, Transmission across chemical synapses, neurotransmitter receptors and postsynaptic signal transmission, Activation of NMDA receptors and postsynaptic events	RRAS
Neuronal system, Potassium channels	KCNMA1, KCNK2

Table 5. Differentially Expressed Genes in GMSCs in Hypoxic Preconditioning Belonging to REACTOME Pathway Related to Developmental Biology and Nervous System.

Pathways	Genes
Developmental biology, Activation of HOX genes during differentiation, Activation of anterior HOX genes in hindbrain development during early embryogenesis	WDR5, MAFB
Developmental biology	MAP2K6, KRT16, NCOA2, FOXO3
Developmental biology, Axon guidance	PRKAR2A, PIK3R3, NRCAM, COL4A2, ITGA10, APH1B, EPHB3, CLASP1
Neuronal system, Transmission across chemical synapses	RASGRF2, RIMS1
Neuronal system, Potassium channels	ABCC9

Table 6. Differentially Expressed Genes in Normoxia Belonging to REACTOME Pathway Related to Developmental Biology and Nervous System.

Pathways	Genes
Developmental biology, Activation of HOX genes during differentiation, Activation of anterior HOX genes in hindbrain development during early embryogenesis	HIST1H2BH, HIST1H3F, HIST1H3E
Developmental biology	CEBPD, SREBF1, NCOA1, PPARA
Developmental biology, Axon guidance	SRGAP3
Neuronal system, Protein-protein interactions at synapses	LRFN4
Neuronal system, Transmission across chemical synapses	ADCY3

because of the breakdown of symmetry and cell polarization[30,31]. We showed that the hypoxic preconditioning influenced the GMSCs transcriptional profile and may improve their neuronal differentiation induced by incubation with a neuroinductive medium. GMSCs differentiated after exposure to hypoxia showed the expression of a higher number of genes with Log2 fold change >2 associated with cortical development compared with those cultured in normoxic conditions.

As expected, the characterization through GO analysis revealed that the genes commonly expressed during differentiation in all samples were correlated with cellular, metabolic, and developmental processes, including nervous system development. Looking at the GO analysis of genes expressed only in one condition, we observed the significant involvement of categories linked to cellular and metabolic processes, but interestingly, only in GMSCs differentiated after hypoxic preconditioning was the GO process "regulation of dendrite development" significantly represented.

Previous reports have shown that hypoxia altered the transcriptional profile of MSCs[32–35]. In particular, gene expression of Wharton's jelly-derived MSCs (WJ-MSCs) cultured in hypoxia and normoxia were compared and different profiles were observed. Different stem cell markers and early mesodermal/endothelial genes showed an increased expression in hypoxia, indicating that culturing WJ-MSCs in hypoxia leads to different development results or the commission to different cells[32]. The influence of hypoxia on the differentiation potential of MSCs is an intriguing argument, and the literature is divided on the subject, with some studies showing an inhibition of differentiation capacity[36,37], while others indicate a better differentiation capacity of MSCs under hypoxic conditions[16,38]. Cicione et al. showed that severe hypoxia reduced the differentiation capacity of bone marrow MSCs (BMSCs) toward the adipogenic, osteogenic, and chondrogenic lineage[36]. Nekanti et al. showed that WJ-MSCs maintained the capacity to undergo osteogenic, adipogenic, and chondrogenic differentiation, but no statistically significant differences were observed compared with cells in normoxia[32]. Our results agree with

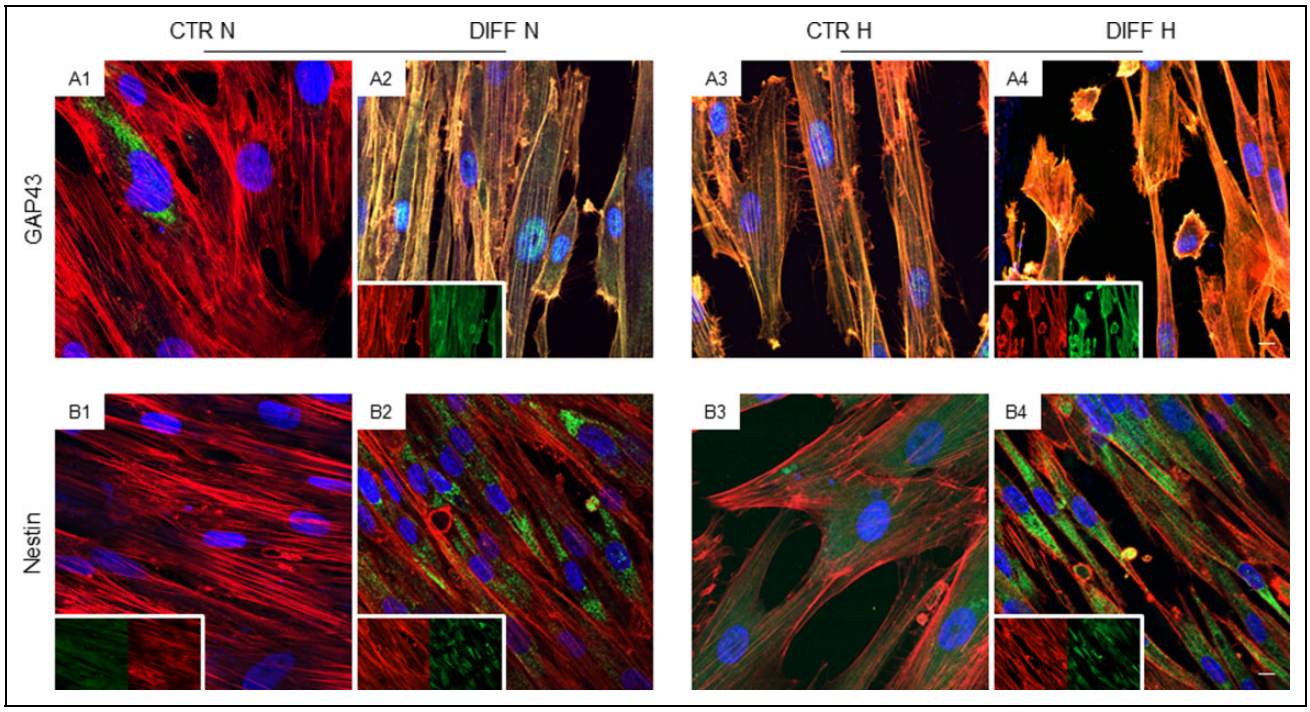

Fig. 5. Neurogenic related markers expression. Immunostaining of GAP43 in undifferentiated GMSCs (A1) and neurogenic differentiated GMSCs (A2) maintained under normoxic conditions. Immunostaining of GAP43 in undifferentiated GMSCs (A3) and neurogenic differentiated GMSCs (A4) after hypoxic preconditioning. Immunostaining of nestin in undifferentiated GMSCs (B1) and neurogenic differentiated GMSCs (B2) maintained under normoxic conditions. Immunostaining of nestin in undifferentiated GMSCs (B3) and neurogenic differentiated GMSCs (B4) after hypoxic preconditioning. Inset shows the separate channel of fluorescence red and green in differentiated samples. Red fluorescence: actin. Green fluorescence: specific markers. Blue fluorescence: nuclei. Scale bar: 5 μm.

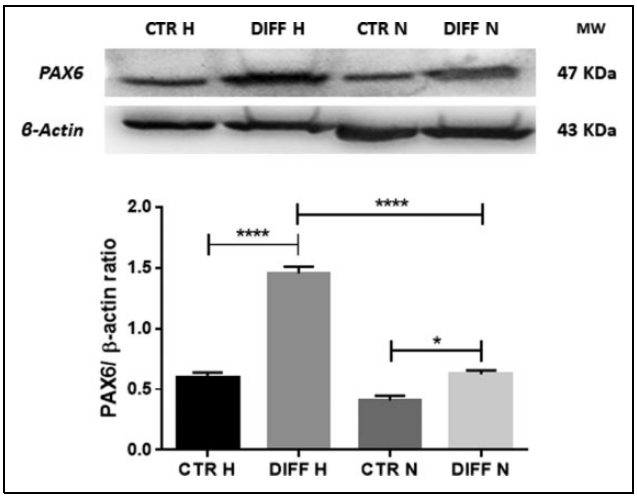

Fig. 6. Western blot and densitometric analysis. PAX6 protein levels were measured in CTR-N, DIFF-N, CTR-H and DIFF-H. Beta-Actin was used as housekeeping protein. *$P < 0.05$; ****$P < 0.0001$.

those studies reporting a better differentiation capacity in hypoxia. Indeed, our results indicated that hypoxia preconditioning increased the expression of genes associated with cortical differentiation at transcriptional level. Moreover, GO and pathway analysis showed that a higher number of genes associated with neuronal differentiation and neuronal system were present in DIFF-H compared with DIFF-N. Furthermore, it was demonstrated that 3% O_2 treatment enhanced rat MSC proliferation, and, during neuronal differentiation, hypoxia enhanced the dopaminergic neuronal differentiation, as demonstrated by the presence of tyrosine hydroxylase (TH)-positive cells. Moreover, hypoxia-induced dopaminergic neurons, obtained from human fetal MSCs, transplanted into parkinsonian rats, improved behavioral impairments[38]. In addition, olfactory mucosa MSCs were induced to differentiate toward dopaminergic neurons by culturing them under hypoxic conditions (3% O_2) in a specific medium. In particular, the differentiated cells showed higher levels of TH and dopamine, together with a slow potassium current[39].

It has been reported that hypoxia induced an up-regulation of neurogenic and osteogenic differentiation genes in MSCs from the apical papilla (SCAP). Moreover, cultured in differentiation medium, SCAP differentiated into neurogenic, osteogenic, and adipogenic lineages in normoxia, but only into neurogenic and osteogenic lineages in hypoxia[40]. In particular, hypoxia increased the neuronal differentiation of SCAP in the presence of differentiation factors[40].

However, Fehrer et al. found that in the hypoxic condition the differentiation capacity of MSCs was diminished, but MSCs preconditioned at 3% O_2 could subsequently be induced to differentiate at 20% O_2[37].

It is important to note that the different results available in the literature may result from the different conditions used in the studies. Different variables are present in the reports, such as the differentiation mediums, the O_2 concentrations, the time of exposure, and if hypoxia was used only as a pretreatment or if the differentiation was carried out at low O_2 concentrations. In particular, regarding O_2 concentration, different studies used various O_2 hypoxic concentrations, varying mainly in the range 1–5%[29,39,41]. Holzwarth et al. reported that 1% O_2 tension reduced adipogenic and osteogenic differentiation, but an increase to 3%, such as in our study, restored osteogenic differentiation[41]. In addition, the donor and the source of MSCs may influence the result. The MSCs used in the study of Cicione et al. were obtained from osteoarthritic patients. Thus it is possible, as suggested by the authors, that those MSCs showed different properties compared with cells isolated from healthy donors[36].

The duration of hypoxia is also a pivotal parameter to consider in order to understand its effects on the properties of MSCs. It was reported that hypoxic MSCs at passage 0 showed a lower number of colonies of small dimension, and cells appeared morphologically undifferentiated and contained fewer mitochondria than those in normoxia[42]. Furthermore, MSCs displayed inhibition of genes involved in DNA metabolism and the cell cycle, while genes involved in adhesion and metabolism were induced. On the contrary, hypoxic MSCs at passage 2 outgrew the cells cultured in normoxia, and showed an induced expression of genes associated with extracellular matrix assembly, and neural, muscle, and epithelial development. GO analysis evidenced the over-representation of a functional group of genes involved in cell plasticity[42], a main property of stem cells[43].

Furthermore, in our study we only preconditioned GMSCs for 48 h in hypoxia before differentiation. Elabd et al. showed that hypoxia preconditioning enhanced the MSCs' differentiation potential toward adipocyte and chondrocyte lineages[35].

It was reported that hypoxic preconditioning increased the dimension and the number of neurospheres in BMSCs[44]. However, hypoxia did not alter the ability of neurospheres to form neuron and glia precursors. In addition, Schwann cell-like cells obtained from hypoxia-preconditioned BMSCs expressed S100β /p75 and the ability for myelination in vitro[44].

We evaluated the expression of the neural stem cell markers nestin and PAX6 and of the synaptic marker GAP43[45]. We observed that CTR-N expressed low levels of GAP43. Interestingly, CTR-H expressed a strong positivity for GAP43 compared with CTR-N. In CTR-N we found low positivity for nestin, while CTR-H showed a stronger positivity for nestin. In DIFF-H both GAP43 and nestin protein levels increased compared with DIFF-N. These data underlined that hypoxia preconditioning enhanced the neuronal differentiation of GMSCs. The increased levels of nestin in hypoxia are in line with the result reported by Wang et al., who observed that nestin expression was higher in the 3% O_2 group after neuronal induction[38]. Also, Kheirandish et al. demonstrated that hypoxia preconditioning increased proliferation and induced the up-regulation of GFAP and a slight increase in the gene expression of nestin in umbilical cord blood MSCs[46]. Moreover, ectodermal PAX6, a transcription factor involved during embryonic development and in eye and brain development[47,48], was up-regulated in DIFF-N and remarkably in DIFF-H as observed by means western blotting analysis. However, hypoxia could ameliorate the properties of MSCs and thus their efficacy in the regenerative medicine field. Indeed, hypoxia improved the proliferation and migration ability of MSCs and induced the secretion of many growth factors[49]. Moreover, hypoxic preconditioning in BMSCs may improve their survival and their regenerative potential[50]. Hypoxia preconditioning up-regulated HIF-1α and growth factors in BMSCs, such as brain-derived neurotrophic factor (BDNF), glial cell-derived neurotrophic factor (GDNF), and vascular endothelial growth factor (VEGF), while many proinflammatory cytokines were downregulated[50]. In addition, hypoxia-preconditioned BMSCs suppressed microglia activity and enhanced neurogenesis in rats subjected to cerebral artery occlusion. Furthermore, animals that received hypoxia-preconditioned BMSCs showed better locomotion recovery compared with stroke control and normoxic BMSCs[50]. Also, data in vivo showed that hypoxia-preconditioned MSCs may be a promising therapeutic approach. Hypoxia-preconditioned MSCs transplanted in a rat model of cardiac arrest-induced global cerebral ischemia enhanced the migration and integration of MSCs and reduced neuronal death and inflammation in the ischemic cortex[51].

In conclusion, hypoxia preconditioning of GMSCs enhanced the transcription of genes involved in neuronal and cortical differentiation, indicating a specific and better differentiation capacity of cells cultured in hypoxia before differentiation. Moreover, a marked positive expression of nestin, PAX6, and GAP43 indicated their commitment toward the neuronal lineage. These results suggest that hypoxia preconditioning could be a useful method to improve MSC properties and neuronal differentiation potential for the treatment of neurodegenerative disorders and in those cases in which neuroregeneration is needed.

Ethical Approval

Written approval for gingival biopsy collection was obtained from the Medical Ethics Committee at the Medical School, "G. d'Annunzio" University, Italy.

Statement of Human and Animal Rights

All procedures in this study were conducted in accordance with the Medical Ethics Committee at the Medical School, "G. d'Annunzio"

University, Italy approved protocols. This article does not contain any studies with animal subjects.

Statement of Informed Consent

Written informed consent was obtained from the patients for gingival biopsy collection.

Declaration of Conflicting Interests

The author(s) declared no potential conflicts of interest with respect to the research, authorship, and/or publication of this article.

Funding

The author(s) disclosed receipt of the following financial support for the research and/or authorship of this article: This work was supported by current research funds 2018 of IRCCS "Centro Neurolesi Bonino Pulejo".

Supplemental Material

Supplemental material for this article is available online.

References

1. Gao L, Xu W, Li T, Chen J, Shao A, Yan F, Chen G. Stem cell therapy: a promising therapeutic method for intracerebral hemorrhage. Cell Transplant. 2018;27(12):1809–1824.
2. Lo Furno D, Mannino G, Giuffrida R. Functional role of mesenchymal stem cells in the treatment of chronic neurodegenerative diseases. J Cell Physiol. 2018;233(5):3982–3999.
3. Rajan TS, Giacoppo S, Diomede F, Ballerini P, Paolantonio M, Marchisio M, Piattelli A, Bramanti P, Mazzon E, Trubiani O. The secretome of periodontal ligament stem cells from MS patients protects against EAE. Sci Rep. 2016;6:38743.
4. Diomede F, Zini N, Gatta V, Fulle S, Merciaro I, D'Aurora M, La Rovere RM, Traini T, Pizzicannella J, Ballerini P, Caputi S, et al. Human periodontal ligament stem cells cultured onto cortico-cancellous scaffold drive bone regenerative process. Eur Cell Mater. 2016;32:181–201.
5. Cianci E, Recchiuti A, Trubiani O, Diomede F, Marchisio M, Miscia S, Colas RA, Dalli J, Serhan CN, Romano M. Human periodontal stem cells release specialized proresolving mediators and carry immunomodulatory and prohealing properties regulated by lipoxins. Stem Cells Transl Med. 2016;5(1):20–32.
6. Chalisserry EP, Nam SY, Park SH, Anil S. Therapeutic potential of dental stem cells. J Tissue Eng. 2017;8:2041731417702531.
7. Fournier BP, Larjava H, Hakkinen L. Gingiva as a source of stem cells with therapeutic potential. Stem Cells Dev. 2013;22(24):3157–3177.
8. Diomede F, Gugliandolo A, Cardelli P, Merciaro I, Ettorre V, Traini T, Bedini R, Scionti D, Bramanti A, Nanci A, Caputi S, et al. Three-dimensional printed PLA scaffold and human gingival stem cell-derived extracellular vesicles: a new tool for bone defect repair. Stem Cell Res Ther. 2018;9(1):104.
9. Gugliandolo A, Diomede F, Cardelli P, Bramanti A, Scionti D, Bramanti P, Trubiani O, Mazzon E. Transcriptomic analysis of gingival mesenchymal stem cells cultured on 3D bioprinted scaffold: a promising strategy for neuroregeneration. J Biomed Mater Res A. 2018;106(1):126–137.
10. Diomede F, Rajan TS, Gatta V, D'Aurora M, Merciaro I, Marchisio M, Muttini A, Caputi S, Bramanti P, Mazzon E, Trubiani O. Stemness maintenance properties in human oral stem cells after long-term passage. Stem Cells Int. 2017;2017:5651287.
11. Fawzy El-Sayed KM, Dorfer CE. Gingival mesenchymal stem/progenitor cells: a unique tissue engineering gem. Stem Cells Int. 2016;2016:7154327.
12. Haque N, Rahman MT, Abu Kasim NH, Alabsi AM. Hypoxic culture conditions as a solution for mesenchymal stem cell based regenerative therapy. ScientificWorldJournal 2013;2013:632972.
13. Simon MC, Keith B. The role of oxygen availability in embryonic development and stem cell function. Nat Rev Mol Cell Biol. 2008;9(4):285–296.
14. Ejtehadifar M, Shamsasenjan K, Movassaghpour A, Akbarzadehlaleh P, Dehdilani N, Abbasi P, Molaeipour Z, Saleh M. The effect of hypoxia on mesenchymal stem cell biology. Adv Pharm Bull. 2015;5(2):141–149.
15. Jiang CM, Liu J, Zhao JY, Xiao L, An S, Gou YC, Quan HX, Cheng Q, Zhang YL, He W, Wang YT, et al. Effects of hypoxia on the immunomodulatory properties of human gingiva-derived mesenchymal stem cells. J Dent Res. 2015;94(1):69–77.
16. Kwon SY, Chun SY, Ha YS, Kim DH, Kim J, Song PH, Kim HT, Yoo ES, Kim BS, Kwon TG. Hypoxia Enhances cell properties of human mesenchymal stem cells. Tissue Eng Regenerat Med. 2017;14(5):595–604.
17. Libro R, Scionti D, Diomede F, Marchisio M, Grassi G, Pollastro F, Piattelli A, Bramanti P, Mazzon E, Trubiani O. Cannabidiol modulates the immunophenotype and inhibits the activation of the inflammasome in human gingival mesenchymal stem cells. Front Physiol. 2016;7:559.
18. Diomede F, Gugliandolo A, Scionti D, Merciaro I, Cavalcanti MF, Mazzon E, Trubiani O. Biotherapeutic effect of gingival stem cells conditioned medium in bone tissue restoration. Int J Mol Sci. 2018;19(2):E329.
19. Perfetto SP, Ambrozak D, Nguyen R, Chattopadhyay P, Roederer M. Quality assurance for polychromatic flow cytometry. Nat Protoc. 2006;1(3):1522–1530.
20. Diomede F, Rajan TS, D'Aurora M, Bramanti P, Merciaro I, Marchisio M, Gatta V, Mazzon E, Trubiani O. Stemness characteristics of periodontal ligament stem cells from donors and multiple sclerosis patients: a comparative study. Stem Cells Int. 2017;2017:1606125.
21. Trubiani O, Guarnieri S, Diomede F, Mariggio MA, Merciaro I, Morabito C, Cavalcanti MF, Cocco L, Ramazzotti G. Nuclear translocation of PKCalpha isoenzyme is involved in neurogenic commitment of human neural crest-derived periodontal ligament stem cells. Cell Signal. 2016;28(11):1631–1641.
22. Diomede F, D'Aurora M, Gugliandolo A, Merciaro I, Ettorre V, Bramanti A, Piattelli A, Gatta V, Mazzon E, Fontana A, Trubiani O. A novel role in skeletal segment regeneration of

extracellular vesicles released from periodontal-ligament stem cells. Int J Nanomedicine. 2018;13:3805–3825.
23. Diomede F, Zingariello M, Cavalcanti M, Merciaro I, Pizzicannella J, De Isla N, Caputi S, Ballerini P, Trubiani O. MyD88/ERK/NFkB pathways and pro-inflammatory cytokines release in periodontal ligament stem cells stimulated by Porphyromonas gingivalis. Eur J Histochem. 2017;61(2):2791.
24. Ballerini P, Diomede F, Petragnani N, Cicchitti S, Merciaro I, Cavalcanti M, Trubiani O. Conditioned medium from relapsing-remitting multiple sclerosis patients reduces the expression and release of inflammatory cytokines induced by LPS-gingivalis in THP-1 and MO3.13 cell lines. Cytokine. 2017;96:261–272.
25. Rajan TS, Giacoppo S, Trubiani O, Diomede F, Piattelli A, Bramanti P, Mazzon E. Conditioned medium of periodontal ligament mesenchymal stem cells exert anti-inflammatory effects in lipopolysaccharide-activated mouse motoneurons. Exp Cell Res. 2016;349(1):152–161.
26. van de Leemput J, Boles NC, Kiehl TR, Corneo B, Lederman P, Menon V, Lee C, Martinez RA, Levi BP, Thompson CL, Yao S, et al. CORTECON: a temporal transcriptome analysis of in vitro human cerebral cortex development from human embryonic stem cells. Neuron. 2014;83(1):51–68.
27. Zhao Y, Wei ZZ, Zhang JY, Zhang Y, Won S, Sun J, Yu SP, Li J, Wei L. GSK-3beta inhibition induced neuroprotection, regeneration, and functional recovery after intracerebral hemorrhagic stroke. Cell Transplant. 2017;26(3):395–407.
28. Turcato F, Kim P, Barnett A, Jin Y, Scerba M, Casey A, Selman W, Greig NH, Luo Y. Sequential combined treatment of pifithrin-alpha and posiphen enhances neurogenesis and functional recovery after stroke. Cell Transplant. 2018;27(4): 607–621.
29. Ahmed NE, Murakami M, Kaneko S, Nakashima M. The effects of hypoxia on the stemness properties of human dental pulp stem cells (DPSCs). Sci Rep. 2016;6:35476.
30. da Silva JS, Dotti CG. Breaking the neuronal sphere: regulation of the actin cytoskeleton in neuritogenesis. Nat Rev Neurosci. 2002;3(9):694–704.
31. Compagnucci C, Piemonte F, Sferra A, Piermarini E, Bertini E. The cytoskeletal arrangements necessary to neurogenesis. Oncotarget. 2016;7(15):19414–19429.
32. Nekanti U, Dastidar S, Venugopal P, Totey S, Ta M. Increased proliferation and analysis of differential gene expression in human Wharton's jelly-derived mesenchymal stromal cells under hypoxia. Int J Biol Sci. 2010;6(5):499–512.
33. Ohnishi S, Yasuda T, Kitamura S, Nagaya N. Effect of hypoxia on gene expression of bone marrow-derived mesenchymal stem cells and mononuclear cells. Stem Cells. 2007;25(5): 1166–1177.
34. Hu X, Wu R, Shehadeh LA, Zhou Q, Jiang C, Huang X, Zhang L, Gao F, Liu X, Yu H, Webster KA, et al. Severe hypoxia exerts parallel and cell-specific regulation of gene expression and alternative splicing in human mesenchymal stem cells. BMC Genomics. 2014;15:303.
35. Elabd C, Ichim TE, Miller K, Anneling A, Grinstein V, Vargas V, Silva FJ. Comparing atmospheric and hypoxic cultured mesenchymal stem cell transcriptome: implication for stem cell therapies targeting intervertebral discs. J Transl Med. 2018;16(1):222.
36. Cicione C, Muinos-Lopez E, Hermida-Gomez T, Fuentes-Boquete I, Diaz-Prado S, Blanco FJ. Effects of severe hypoxia on bone marrow mesenchymal stem cells differentiation potential. Stem Cells Int. 2013;2013:232896.
37. Fehrer C, Brunauer R, Laschober G, Unterluggauer H, Reitinger S, Kloss F, Gully C, Gassner R, Lepperdinger G. Reduced oxygen tension attenuates differentiation capacity of human mesenchymal stem cells and prolongs their lifespan. Aging Cell. 2007;6(6):745–757.
38. Wang Y, Yang J, Li H, Wang X, Zhu L, Fan M, Wang X. Hypoxia promotes dopaminergic differentiation of mesenchymal stem cells and shows benefits for transplantation in a rat model of Parkinson's disease. Plos One. 2013;8(1):e54296.
39. Zhuo Y, Wang L, Ge L, Li X, Duan D, Teng X, Jiang M, Liu K, Yuan T, Wu P, Wang H, et al. Hypoxic culture promotes dopaminergic-neuronal differentiation of nasal olfactory mucosa mesenchymal stem cells via upregulation of hypoxia-inducible factor-1alpha. Cell Transplant. 2017;26(8): 1452–1461.
40. Vanacker J, Viswanath A, De Berdt P, Everard A, Cani PD, Bouzin C, Feron O, Diogenes A, Leprince JG, des Rieux A. Hypoxia modulates the differentiation potential of stem cells of the apical papilla. J Endod. 2014;40(9):1410–1418.
41. Holzwarth C, Vaegler M, Gieseke F, Pfister SM, Handgretinger R, Kerst G, Muller I. Low physiologic oxygen tensions reduce proliferation and differentiation of human multipotent mesenchymal stromal cells. BMC Cell Biol. 2010;11:11.
42. Basciano L, Nemos C, Foliguet B, de Isla N, de Carvalho M, Tran N, Dalloul A. Long term culture of mesenchymal stem cells in hypoxia promotes a genetic program maintaining their undifferentiated and multipotent status. BMC Cell Biol. 2011; 12:12.
43. Zipori D. The stem state: plasticity is essential, whereas self-renewal and hierarchy are optional. Stem Cells. 2005;23(6): 719–726.
44. Mung KL, Tsui YP, Tai EW, Chan YS, Shum DK, Shea GK. Rapid and efficient generation of neural progenitors from adult bone marrow stromal cells by hypoxic preconditioning. Stem Cell Res Ther. 2016;7(1):146.
45. Jang S, Cho HH, Cho YB, Park JS, Jeong HS. Functional neural differentiation of human adipose tissue-derived stem cells using bFGF and forskolin. BMC Cell Biol. 2010;11:25.
46. Kheirandish M, Gavgani SP, Samiee S. The effect of hypoxia preconditioning on the neural and stemness genes expression profiling in human umbilical cord blood mesenchymal stem cells. Transfus Apher Sci. 2017;56(3):392–399.
47. Yan Q, Gong L, Deng M, Zhang L, Sun S, Liu J, Ma H, Yuan D, Chen PC, Hu X, Liu J, et al. Sumoylation activates the transcriptional activity of Pax-6, an important transcription factor for eye and brain development. Proc Natl Acad Sci U S A. 2010;107(49):21034–21039.
48. Diomede F, Zini N, Pizzicannella J, Merciaro I, Pizzicannella G, D'Orazio M, Piattelli A, Trubiani O. 5-aza exposure

improves reprogramming process through embryoid body formation in human gingival stem cells. Front Genet. 2018;9:419.
49. Hung SP, Ho JH, Shih YR, Lo T, Lee OK. Hypoxia promotes proliferation and osteogenic differentiation potentials of human mesenchymal stem cells. J Orthop Res. 2012;30(2):260–266.
50. Wei L, Fraser JL, Lu ZY, Hu X, Yu SP. Transplantation of hypoxia preconditioned bone marrow mesenchymal stem cells enhances angiogenesis and neurogenesis after cerebral ischemia in rats. Neurobiol Dis. 2012;46(3):635–645.
51. Wang JW, Qiu YR, Fu Y, Liu J, He ZJ, Huang ZT. Transplantation with hypoxia-preconditioned mesenchymal stem cells suppresses brain injury caused by cardiac arrest-induced global cerebral ischemia in rats. J Neurosci Res. 2017;95(10): 2059–2070.